

Point defects in pure amorphous silicon and their role in structural relaxation: A tight-binding molecular-dynamics study

Xavier Urli, Cristiano L. Dias,* Laurent J. Lewis,† and Sjoerd Roorda

Département de Physique et Regroupement Québécois sur les Matériaux de Pointe (RQMP), Université de Montréal, Case Postale 6128, Succursale Centre-Ville, Montréal, Québec, Canada H3C 3J7

(Received 20 August 2007; revised manuscript received 7 December 2007; published 9 April 2008)

Structural relaxation in pure amorphous silicon (*a*-Si) produced by ion implantation has been attributed to the annihilation of point defects (vacancies and interstitials) introduced during the amorphization process. We have studied this problem by using tight-binding molecular-dynamics simulations. We find that structural defects can, indeed, be identified in *a*-Si—they manifest themselves through a strong correlation between the charge and the volume of nearby atoms. The relaxation of these defects proceeds via the recombination of the dangling bonds. This results in an increase in the coordination number at constant density; the relaxation of *a*-Si, therefore, results from local, rather than global, structural changes, in full agreement with the high-precision x-ray diffraction experiments of Laaziri *et al.* [Phys. Rev. Lett. **82**, 3460 (1999)].

DOI: [10.1103/PhysRevB.77.155204](https://doi.org/10.1103/PhysRevB.77.155204)

PACS number(s): 61.43.Dq, 61.43.Bn, 71.55.Jv

I. INTRODUCTION

The amorphous phase of tetrahedral covalent semiconductors—and most notably amorphous silicon (*a*-Si)—has often been described in terms of the ideal continuous random network (CRN),¹ which is fully connected and perfectly fourfold coordinated. In the CRN, the angular and radial distributions of atoms resemble those of the corresponding crystalline materials at short range; disorder accumulates at longer range and, in practice, very little sign of crystallinity is found past the third or fourth neighbor shell. That being said, the atomic structure of these materials has not yet been completely resolved and the analogy with the CRN has not been fully established. In particular, there exists no evidence that the coordination number of the prototypical *a*-Si is equal to 4, even though computer models do indicate that this might very well be the case;² experiment has not yet been able to provide a definite answer to this question (but see below).

In this context, the presence of point defects and their role during structural relaxation have been the object of several investigations. A striking similarity has been noted between the changes induced in *a*-Si by annealing and those associated with the removal of damage caused by radiation in crystalline Si (*c*-Si).³ This has led to the idea that point defects such as vacancies and interstitials do exist in *a*-Si, and these are closely related to structural relaxation. Evidence for this arises from measurements of the kinetics of heat released upon annealing,³ Mössbauer spectroscopy,⁴ Cu solubility and diffusion,⁵ and high-energy x-ray diffraction (XRD).⁶ In the latter, the radial distribution function (RDF) of *pure*, ion-implanted *a*-Si was measured with very high precision, both before (i.e., as-implanted) and after annealing. The two states of the material were observed to be undercoordinated and *equally dense*; however, the average coordination number was found to increase from 3.79 to 3.88 upon annealing. This, as well as other details of the RDFs, was interpreted in terms of the mutual annihilation of vacancies and interstitials during relaxation, which brings about an increase in the average coordination number without affecting the density. It is

important to note that the increase in the coordination number during annealing is very significant and does indicate that structural defects play a role in the annealing process.

Though perhaps not completely intuitive, the concept of topological defects provides an interesting approach to understanding the structure (and structural relaxation) of amorphous semiconductors. (Point defects have also been invoked in the context of *a*-Si/*c*-Si interface studies—see, for instance, Ref. 7.) However, questions remain before this interpretation can be fully accepted. In particular, can theory provide a direct evidence of the existence of point defects in these materials? How are they related to structural relaxation? What are the structural and electronic properties of vacancies and interstitials in amorphous semiconductors? In this paper, we demonstrate, based on quantum-mechanical tight-binding simulations, that the interpretation of structural relaxation in *a*-Si in terms of point defects (here, we take vacancies as a case study) is very plausible. We propose a specific criterion for identifying vacancies, namely, an anomalous volume-charge relation, and show that the changes in the RDF observed in the XRD experiments can be explained if defects are assumed to exist and to annihilate.

II. COMPUTATIONAL DETAILS

The starting point of the present study is a CRN model containing 216 atoms prepared using a modified Wooten–Winer–Weaire (WWW) algorithm² together with the empirical (or classical) Stillinger–Weber potential.⁸ Since classical potentials provide no information on the electronic structure of the materials, a quantum-mechanical approach is required to proceed further. We used the tight-binding molecular dynamics (TBMD) (see, e.g., Ref. 9) scheme, which ensures a proper—and “affordable”—description of the structural energetics of the material, while also providing information on the electronic structure; *ab initio* simulations are out of reach for the present purposes, as large cells and relatively long simulation times are needed.

TBMD provides a method for computing the electronic properties of materials in terms of a set of parameters de-

scribing the overlap between atomic orbitals on neighboring atoms. The total energy is expressed as

$$E[n(\mathbf{r})] = \sum_{\text{occ.}} \epsilon_s + F[n(\mathbf{r})], \quad (1)$$

where the first term is the “band-structure” energy—the sum is over occupied states—and the second term accounts for all other contributions to the total energy, including the nuclear-nuclear repulsion. The particular implementation of TBMD we used is that of Cohen *et al.*,¹⁰ which is parametrized for silicon by Bernstein *et al.*,¹¹ full details can be found in Ref. 12. While fitted to a small number of high-symmetry crystalline structures, this model has been shown to describe remarkably well such properties as elastic constants, phonon frequencies, and, most important for our purposes, point defect formation energies in *c*-Si. Also, it correctly accounts for the energy sequence of various adatom configurations and surface reconstructions.¹¹ In addition, the model provides a very good description of the electronic structure of *a*-Si, in particular, in the presence of surfaces where defects abound.¹¹ Finally, the model has been shown to yield *a*-Si structures and vibrational properties in excellent agreement with both *ab initio* and experimental results.¹³ Thus, the model evidently captures the essential physics of bonding in both *a*-Si and *c*-Si.

The total energy is rewritten

$$E[n(\mathbf{r})] = \sum_{\text{occ.}} \epsilon'_s, \quad (2)$$

where the $\epsilon'_s = \epsilon_s + F[n(\mathbf{r})]/N_e$ are the “shifted” eigenvalues and N_e is the number of electrons. These are obtained from a parametrized local-atomic-orbital representation of the Hamiltonian. The electronic wave functions centered on atom i for the state s are expanded in terms of a reduced number of localized basis functions

$$|\psi_i^{(s)}\rangle = \sum_{\alpha} c_{i\alpha}^{(s)} |\phi_{\alpha}\rangle, \quad (3)$$

where the coefficients are obtained by solving

$$\sum_{j\beta} (H_{i\alpha j\beta} - \epsilon^{(s)} S_{i\alpha j\beta}) c_{j\beta}^{(s)} = 0, \quad (4)$$

where H is the on-site Hamiltonian and S the overlap. The basis set $|\phi_{\alpha}\rangle$ uses the single $3s$ and the three $3p$ orbitals.

The WWW model described above was fully relaxed using TBMD so as to bring it to its lowest-energy amorphous state. It is an excellent representation of ideal *a*-Si: it is perfectly coordinated ($Z=4$) and the root-mean-square variations of the nearest-neighbor distance and the bond-angle distributions are a minuscule 0.07 Å and 9.55°, respectively, which compare very favorably with other models in the literature as can be seen in Table I.

In order to assess the role of point defects on relaxation, “as-made” (or as-implanted) samples were prepared by manually introducing point defects—in this case vacancies—in the fully relaxed WWW sample. A vacancy is created by removing one atom from its equilibrium position, thus leading to the creation of four dangling bonds. In practice, only one defect is introduced at a time in the 216-atom

TABLE I. Comparison of the properties of the initial TBMD-relaxed WWW model with other models (Ref. 9) and with experiment (Ref. 3): atomic density ρ , coordination number Z , average nearest-neighbor distance \bar{r} , and average bond angle $\bar{\theta}$. For crystalline silicon, $Z=4$, $\bar{r}=2.355$, and $\bar{\theta}=109.47^\circ$.

	Value	rms deviation	Models	Experiment
ρ (at/Å ³)	0.04743			0.0489
Z	4.00		3.98	3.88
\bar{r} (Å)	2.39	0.07		2.35
$\bar{\theta}$ (deg)	109.25	9.55	109.4	109.3

network, leading to a density of threefold coordinated defects of about 1.8%, which is consistent with the values from experiment.³ In order to obtain statistically meaningful results, all 216 possible configurations (one for each atom) were examined. The system was relaxed using a conjugate-gradient scheme after the introduction of each defect so as to let the atoms find their most favorable positions.

The as-made sample was then fully relaxed in order to eliminate the defects in a way that is analogous to experiment. This was done by running first at 300 K for 3 ps, cooling to 0 K at a rate of 10^{14} K/s, and subjecting the system to a final conjugate-gradient minimization in order to remove any remaining strain. This model will be identified with the fully annealed material of the XRD experiments in what follows. We stress here that our study is concerned with pure *a*-Si, as opposed to hydrogenated amorphous silicon; pure *a*-Si is experimentally prepared by implanting highly energetic Si ions in *c*-Si, which disorder and amorphize the structure. This material—probably the closest experimental realization of the ideal CRN—contains essentially no impurities and the energy gap is free of defects.

It is important to note that our purpose here is to examine the role of defects on the structure and electronic properties of *a*-Si. To this end, we must dispose of a well-defined, strain-free structure that will allow precise monitoring of the changes induced by the defects in well-controlled states of the system. Thus, whether or not the WWW CRN represents “real-life” *a*-Si precisely is not a key issue here; in fact, constructing proper models of *a*-Si is the object of numerous ongoing efforts well beyond the scope of our work. Experimentally, the coordination number increases by 0.09 upon annealing; this change is significant and is a definite signature of the presence of defects as our model clearly demonstrates.

A typical defect configuration is presented in Fig. 1. The atoms surrounding the vacancy (within ~ 3 Å) will be referred to as “neighbors”; they will be examined in detail so as to provide information on the role of defects during structural relaxation. Turning the problem around, it is necessary to be able to locate defects with reasonable confidence *without a priori knowledge of their position* in order to demonstrate their existence. This is not a trivial enterprise: because disorder is not “uniform,” no criterion can provide a perfect answer and there always will be marginal cases. A criterion based solely on distance—e.g., identification of clusters of

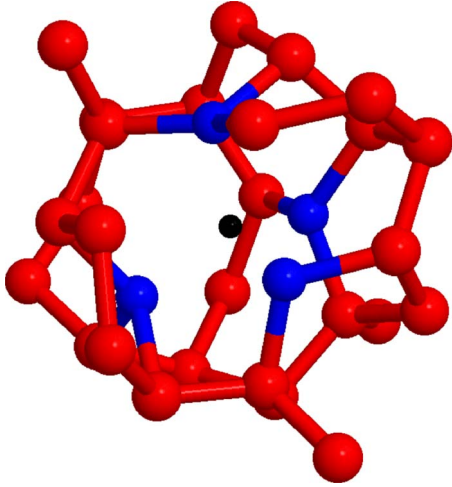


FIG. 1. (Color online) A typical defect configuration. The vacancy (position of the atom which has been removed) is indicated by the small black sphere; the blue (dark gray) spheres are the nearest-neighbor atoms and the red (medium gray) spheres are more distant atoms. Note that this color code is used in all plots and figures.

threefold atoms, which may signify the presence of a vacancy—is not sufficiently robust for this purpose. We demonstrate below that it is possible to identify defects by looking for *correlations* between local properties; the assumption, which we have verified, is that the presence of a defect is more strongly felt at short range. In particular, defects have a sizable effect on the volume available to neighboring atoms¹⁴ as well as on their charges.

III. RESULTS

A. Role and identification of structural defects

We first discuss the effect of the presence of defects on structural and electronic properties; more precisely, we investigate ways of identifying (and thus establishing the existence of) topological defects in *a*-Si. As mentioned above, defects have hardly perceptible effects on such properties as bond-length distribution, bond-angle distribution, and dihedral-angle distribution, which all depend in some way on the distances between the vacancy and nearby atoms. We also considered the distribution of Voronoi volumes, which are expected to be significantly larger around a defect; *per se*, this quantity does not provide an unambiguous evidence of the presence of defects because it is widely distributed—large volumes are found everywhere in the system. Taken in correlation with electronic properties, however, the Voronoi volume does provide the identification criterion we are seeking; we will return to this point below, but first we discuss the electronic signature of defects.

There are three electronic quantities that are relevant to the present problem: (i) the actual charge on the atoms:

$$Q_i = 2 \sum_{s=1}^{\text{occ.}} \sum_{\alpha} (c_{i\alpha}^{(s)})^2, \quad (5)$$

TABLE II. Average charges Q_s , Q_p , and Q_{tot} for the perfect, reference *a*-Si model (which is akin to the annealed sample) and for various categories of atoms in the defective model (as-implanted): first nearest neighbors to vacancies, second nearest neighbors to vacancies, and others. The numbers in parentheses are the rms variations.

	Perfect	Defective		
		1st NN	2nd NN	Others
Q_s	1.55 (0.02)	1.70 (0.04)	1.55 (0.02)	1.55 (0.04)
Q_p	2.45 (0.05)	2.52 (0.18)	2.44 (0.05)	2.44 (0.05)
Q_{tot}	4.00 (0.04)	4.22 (0.20)	3.99 (0.04)	3.99 (0.04)

(ii) the local density of states (LDOS):

$$n_i(E) = \sum_s |\psi_i^{(s)}|^2 \delta(E - \epsilon_s) = \sum_s \sum_{\alpha} c_{i\alpha}^{(s)} \delta(E - \epsilon_s) c_{i\alpha}^{(s)}, \quad (6)$$

and (iii) the bond-order parameter:

$$\eta_i = \sum_{j \neq i} \sum_{\alpha\beta} \rho_{i\alpha j\beta}, \quad (7)$$

where $\rho_{i\alpha j\beta}$ is the density matrix.

The average charges (projected on the *s* and *p* orbitals) for the perfect (“annealed”) configuration, as well as for three different types of atoms in the defective (“as-implanted”) configurations, are presented in Table II. In the presence of defects, the atoms that are close neighbors to the vacancies evidently suffer a significant increase in their overall charge (by about 5%), and this mostly affects the *s* orbitals ($\sim +15\%$); atoms which are second nearest neighbors and beyond are essentially unaffected. The effect is even more clearly evident in the distribution of charges, as presented in Fig. 2: the distribution of *s* charges for nearest neighbors, peaking at ~ 1.7 , is almost completely detached from that for other atoms, while *p* charges (as well as the total charge) are much more widely distributed for nearest neighbors. Thus, it would appear that the *s* charge, Q_s , provides an indication of the presence of defects, at least from the electronic viewpoint. (Note that, in all plots, the distributions have been normalized to 1 to ease comparison; the distributions should in effect be multiplied by the number of atoms they involve.)

It is known that defects introduce states in the gap of amorphous semiconductors^{15–18} and can thus presumably be detected by examining their contribution to the spectrum of electronic states. The LDOS provides a measure of the importance of local states in the overall density of states (DOS). Figure 3 shows the relative contributions of the different types of atoms to gap states for our defective structures. Again here, atoms neighboring vacancies behave in a peculiar manner, essentially because they are affected by dangling bonds.^{16,19,20} (The DOS for the reference sample is almost free of gap states.) This feature is, however, not unambiguous: a number of “ordinary” atoms contribute significantly to

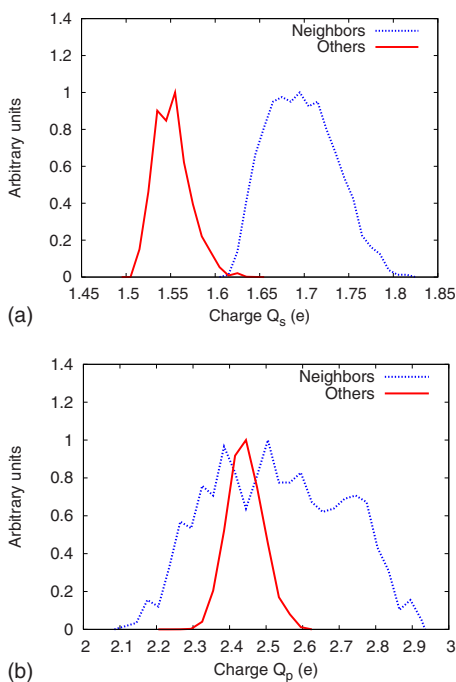


FIG. 2. (Color online) Normalized distributions of charges (a) Q_s and (b) Q_p for all atoms in the as-made samples.

the gap.⁹ Those ordinary atoms could, for instance, have a strongly strained local environment that would induce electronic states in the gap.¹⁸

A purely electronic signature, therefore, does not provide conclusive evidence of the existence of structural defects. Intuition strongly suggests, however, that electronic defects must leave topological traces. Likewise, the disordered nature of the amorphous structure prevents the identification of structural defects on the basis of a topological criterion alone. As we demonstrate next, it is in the correlation between the two measures—electronic and structural—where the answer lies.

We show in Fig. 4(a) the relation between charge and volume for all atoms in a particular configuration (depicted) of an as-implanted sample containing a defect. Most of the points fall into a well-defined region of this “phase diagram”; there are four exceptions, however, corresponding to the four atoms that surround the vacancy. The well-defined region shows a strong correlation where the charge decreases with

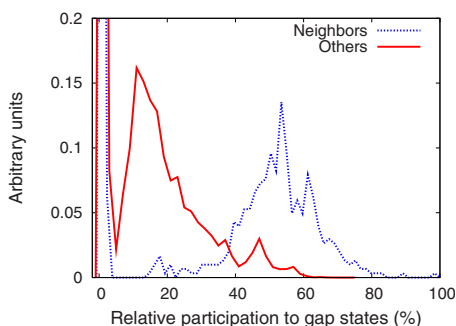


FIG. 3. (Color online) Participation of neighbors and other atoms to gap states, as indicated, for the as-made samples.

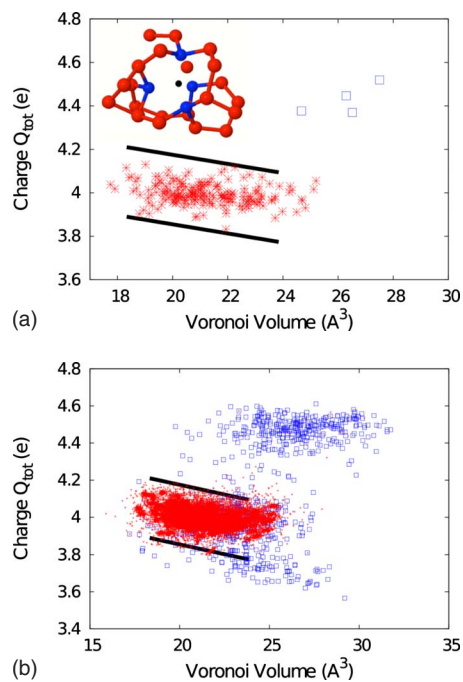


FIG. 4. (Color online) Charge-volume correlation for (a) the particular defective configuration depicted and (b) the ensemble of defective configurations (as-made samples). The blue (dark gray) squares are for neighbors and the red (medium gray) stars or crosses are for other atoms. The lines are a guide for the eye and are the same in both panels.

the volume. This can be understood as follows: small Voronoi volumes are related to large nuclear-nuclear repulsion, which can only lead to stable structures if screened by a large amount of electron.²¹ An amalgamated plot for all defective configurations is presented in Fig. 4(b). The result is very similar, albeit with a non-negligible “error bar”: by and large, atoms close to the vacancies do *not* obey the normal correlation—they have larger volumes in general, and lie within two reasonably well-defined groups with either an excess (+0.5) or a deficit (−0.2) of charge; the two groups will be referred to as “I” and “II,” respectively. Since these atoms are by construction spatially correlated, this analysis provides the correlation we are seeking between charge, volume, and topology, i.e., the vacancies can be identified and located in space. Of course, the criterion is not absolute, and no criterion seems to be able to provide a fully unambiguous identification. This is really a question of probability (or “level of confidence”); on average, each of the four atoms initially defining the vacancy has a probability of 0.87 to be defective, i.e., to lie outside of the region where the normal charge-volume relation holds.

It is interesting to note that group-I atoms are threefold coordinated and, in general, occupy a larger volume than group-II atoms, which are fivefold coordinated. Thus, vacancies in *a*-Si are associated not only with undercoordinated atoms, but also with a significant number of overcoordinated atoms. (Fivefold coordinated atoms occupy slightly less space than threefold coordinated atoms simply because there are more atoms sharing the same local volume.)

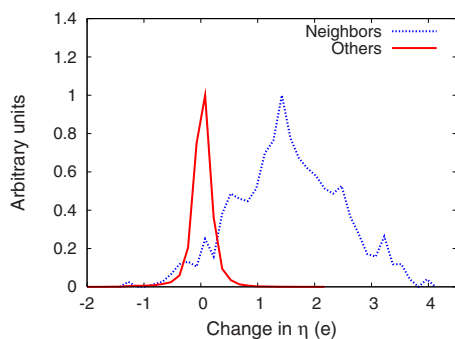


FIG. 5. (Color online) Difference in the bond-order parameter during annealing (i.e., between as-made and annealed samples) for atom neighboring vacancies and others, as indicated.

B. Discussion: Defects and relaxation

Having established that topological defects do exist (and can be identified) in *a*-Si, we move on to examining their role in relaxation. As discussed earlier, the existence of defects was experimentally inferred from an analogy in the annealing kinetics of *a*-Si and *c*-Si, as well as high-precision XRD measurements of the structural changes induced by annealing as-implanted *a*-Si—the coordination number Z was found to increase by 0.09 (from 3.79 to 3.88); as mentioned earlier, this increase in Z is not accompanied by densification. These observations suggest that relaxation comes about from the reconstruction of dangling bonds near vacancies (which, therefore, disappear from the gap); thus, annealing would be the consequence of *local* relaxation effects, not of a *global* relaxation process whereby the whole system becomes “a little more crystalline.” Of course, one piece of evidence for this thesis is the fact that gap states, associated with undercoordinated atoms, do disappear upon relaxation. However, this does not provide a link to topological defects. In fact, the average nearest-neighbor distance and bond-angle distribution change very little during the annealing process. Some atoms do move, and these are associated with vacancies: they have room to do so, and they do so because this allows dangling bonds to reconstruct. The net result is that the coordination increases; our calculations give (by integrating over the first peak of the radial distribution function) $\Delta Z=0.05$ (from 3.94 in the as-made sample to 3.99 in the annealed sample), which is of the same order as the value from experiment ($\Delta Z=0.09$). (This comparison should not be taken *stricto sensu*: in the real material, interstitials are also present in a proportion that is not known precisely; these may recombine with vacancies. Defect recombination and relaxation proceed at constant density and yield an overall increase in the coordination which, however, remains smaller than 4, indicating that residual vacancies are present.)

The bond-order parameter [cf. Eq. (7)] allows for a more precise analysis of the recombination of bonds during annealing and reinforces our findings concerning the identification of topological defects. As can be judged from Fig. 5, the changes are much more pronounced for atoms that are near vacancies ($\Delta\eta=1.55$, with a standard deviation of 0.9) than atoms which are not (average is zero and standard

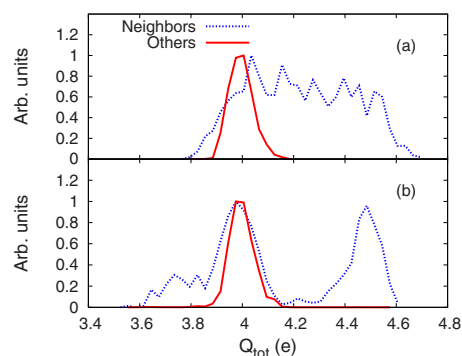


FIG. 6. (Color online) Charge distribution in (a) the as-implanted sample and (b) the relaxed sample.

deviation is 0.2). Thus, atoms neighboring defects increase their bond order by operating bond recombination with nearby atoms, providing further evidence that relaxation or annealing is a local mechanism.

As a result of the creation of new bonds during annealing, the charge on the atoms is expected to change, in particular, on those which are near the defects. The distribution of the charge for all the atoms in the defective systems is displayed in Fig. 6. In the as-implanted sample, the neighbors present a wide, featureless distribution, with an average total charge of 4.22. After annealing, these atoms split into three types, clearly visible in the presence of three humps: normal with charge ~ 4 , increased charge (about +0.5, group-I atoms), and decreased charge (about -0.2 , group-II atoms). A close inspection of the LDOS reveals that group-I atoms are responsible for the gap states that move toward the valence band during annealing, while group-II atoms are associated with states that move toward the conduction band. This provides a mechanism for relaxing the energy since group-I electronic states are occupied and lose energy during relaxation, while group-II states gain energy but are unoccupied. The overall result is that the energy decreases; this phenomenon has also been observed in other calculations^{22,23} as well as *c*-Si surface relaxation.²⁴

IV. CONCLUDING REMARKS

We have used TBMD simulations to study the relaxation of models of pure (ion-implanted) amorphous silicon in the presence of point defects (more precisely, vacancies) in order to assess their existence and role during annealing. We have found that structural defects can, indeed, be identified in *a*-Si: they manifest themselves through a strong correlation between the charge and the volume of those atoms that sit nearby. The relaxation of the defects proceeds via the recombination of the dangling bonds; as a result, the overall coordination number increases while the density remains constant. While not exhaustive, our calculations provide strong support to the experimental interpretation of the XRD data⁶ during annealing in terms of local, rather than global, structural changes, proceeding by the annihilation of point defects.

ACKNOWLEDGMENTS

We are grateful to Normand Mousseau for providing the α -Si model. This work has been supported by grants from the Natural Sciences and Engineering Research Council of

Canada (NSERC) and the *Fonds Québécois de la Recherche sur la Nature et les Technologies* (FQRNT). We are grateful to the *Réseau Québécois de Calcul de Haute Performance* (RQCHP) for generous allocations of computer resources.

*Present address: Department of Applied Mathematics, The University of Western Ontario, Middlesex College, 1151 Richmond St. N., London (ON), Canada N6A 5B7.

†Author to whom correspondence should be addressed; laurent.lewis@umontreal.ca

¹R. Zallen, *The Physics of Amorphous Solids* (Wiley, New York, 1983).

²G. T. Barkema and N. Mousseau, *Phys. Rev. B* **62**, 4985 (2000).

³S. Roorda, W. C. Sinke, J. M. Poate, D. C. Jacobson, S. Dierker, B. S. Dennis, D. J. Eaglesham, F. Spaepen, and P. Fuoss, *Phys. Rev. B* **44**, 3702 (1991).

⁴G. N. van den Hoven, Z. N. Liang, L. Niesen, and J. S. Custer, *Phys. Rev. Lett.* **68**, 3714 (1992).

⁵A. Polman, D. C. Jacobson, S. Coffa, and J. M. Poate, *Appl. Phys. Lett.* **57**, 1230 (1990).

⁶K. Laaziri, S. Kycia, S. Roorda, M. Chicoine, J. L. Robertson, J. Wang, and S. C. Moss, *Phys. Rev. Lett.* **82**, 3460 (1999).

⁷S. A. Harrison, D. Yu, T. F. Edgar, G. S. Hwang, T. A. Kirichenko, and S. K. Banerjee, *J. Appl. Phys.* **96**, 3334 (2004).

⁸F. H. Stillinger and T. A. Weber, *Phys. Rev. B* **31**, 5262 (1985).

⁹L. J. Lewis and N. Mousseau, *Comput. Mater. Sci.* **12**, 210 (1998); L. Colombo, *Riv. Nuovo Cimento* **28**, 1 (2005).

¹⁰R. E. Cohen, M. J. Mehl, and D. A. Papaconstantopoulos, *Phys. Rev. B* **50**, 14694 (1994).

¹¹N. Bernstein, M. J. Mehl, D. A. Papaconstantopoulos, N. I.

Papanicolaou, Martin Z. Bazant, and Efthimios Kaxiras, *Phys. Rev. B* **62**, 4477 (2000).

¹²M. J. Mehl and D. A. Papaconstantopoulos, *Phys. Rev. B* **54**, 4519 (1996).

¹³J. L. Feldman, N. Bernstein, D. A. Papaconstantopoulos, and M. J. Mehl, *Phys. Rev. B* **70**, 165201 (2004).

¹⁴R. Lutz and L. J. Lewis, *Phys. Rev. B* **47**, 9896 (1993).

¹⁵S. Knief, W. von Niessen, and T. Koslowski, *Phys. Rev. B* **58**, 4459 (1998).

¹⁶M. Fornari, M. Peressi, S. de Gironcoli, and A. Baldereschi, *Europhys. Lett.* **47**, 481 (1999).

¹⁷D. A. Drabold, P. A. Fedders, O. F. Sankey, and J. D. Dow, *Phys. Rev. B* **42**, 5135 (1990).

¹⁸P. A. Fedders, D. A. Drabold, and S. Klemm, *Phys. Rev. B* **45**, 4048 (1992).

¹⁹J. L. Mercier and M. Y. Chou, *Phys. Rev. B* **43**, 6768 (1991).

²⁰J. M. Hollender and G. J. Morgan, *J. Phys.: Condens. Matter* **4**, 4473 (1992).

²¹C. L. Dias, M.Sc. thesis, Université de Montréal, 2001.

²²J. Dong and D. A. Drabold, *Phys. Rev. Lett.* **80**, 1928 (1998).

²³E. Kim, Y. H. Lee, C. Chen, and T. Pang, *Phys. Rev. B* **59**, 2713 (1999).

²⁴Walter A. Harrison, *Electronic Structure and Properties of Solids: The Physics of the Chemical Bond* (Dover, New York, 1989).